



HAL
open science

Influence of microwave sintering on electrical properties of BCTZ lead free piezoelectric ceramics

Kelly Orlik, Yannick Lorgouilloux, Pascal Marchet, Anthony Thuault, Mohamed Rguiti, Christian Courtois, Florian Jean

► To cite this version:

Kelly Orlik, Yannick Lorgouilloux, Pascal Marchet, Anthony Thuault, Mohamed Rguiti, et al.. Influence of microwave sintering on electrical properties of BCTZ lead free piezoelectric ceramics. Journal of the European Ceramic Society, 2020, 40 (4), pp.1212-1216. 10.1016/j.jeurceramsoc.2019.12.010 . hal-02550924

HAL Id: hal-02550924

<https://unilim.hal.science/hal-02550924v1>

Submitted on 26 Nov 2024

HAL is a multi-disciplinary open access archive for the deposit and dissemination of scientific research documents, whether they are published or not. The documents may come from teaching and research institutions in France or abroad, or from public or private research centers.

L'archive ouverte pluridisciplinaire **HAL**, est destinée au dépôt et à la diffusion de documents scientifiques de niveau recherche, publiés ou non, émanant des établissements d'enseignement et de recherche français ou étrangers, des laboratoires publics ou privés.

Influence of microwave sintering on electrical properties of BCTZ lead free piezoelectric ceramics

Kelly Orlik^a, Yannick Lorgouilloux^{a,*}, Pascal Marchet^b, Anthony Thuault^a, Florian Jean^a, Mohamed Rguiti^a, Christian Courtois^a

^a Univ. Polytechnique Hauts-de-France, EA 2443 - LMCPA - Laboratoire des Matériaux Céramiques et Procédés Associés, F-59313 Valenciennes, France

^b IRCER - UMR CNRS 7315, Centre Européen de la Céramique, 12 Rue Atlantis, F-87068 Limoges Cedex, France

ABSTRACT

Barium titanate doped with calcium and zirconium (BCTZ) could be used at low temperature to replace lead based piezoelectric ceramics (PZT). The classical way to obtain BCTZ is the solid-state route coupled with conventional sintering, but this step is time-consuming. To reduce the duration of this process, microwave heating was used for sintering. It is a fast sintering method and the heating rate was around 200 °C/min in this study. Slightly better electrical properties with finer microstructures ($d_{33}^* = 706$ pm/V, grain size about 42.1 ± 14.2 μm) were obtained for samples sintered by microwave heating during 50 min compared to the conventional sintering ($d_{33}^* = 622$ pm/V, 22.6 ± 4.4 μm). The main result of this study is that by using microwave heating, the sintering step duration (including heating, dwell time and cooling) was drastically reduced: 1.5 h for microwave sintering against 12.5 h for conventional sintering.

Keywords:

Microwave sintering
Lead-free piezoceramics
BCTZ
Ferroelectric properties
Piezoelectric properties

1. Introduction

Lead based piezoelectric ceramics have been used in many applications (sensors, transducers ...), especially $\text{Pb}(\text{Zr},\text{Ti})\text{O}_3$ (PZT). The scientist community has focused on lead free piezoelectric ceramics since the toxicity of lead was demonstrated [1,2] and the European legislations (REACH [3], RoHS [4], WEEE [5]) advocate the replacement of lead based materials by lead free alternatives. For low temperature applications, barium titanate doped with calcium and zirconium has been studied for 10 years [6] and could be a promising candidate to replace PZT based materials. The composition $\text{Ba}_{0.85}\text{Ca}_{0.15}\text{Ti}_{0.90}\text{Zr}_{0.10}\text{O}_3$ (BCTZ) exhibits a high piezoelectric constant, d_{33} reaching 620 pC/N [6], but a low Curie temperature (around 83 °C). The solid state route coupled with conventional sintering has been the classical way to obtain this ceramic with high piezoelectric properties [7]. Other synthesis routes such as sol gel [8,9], combustion [10] and hydrothermal [11,12] methods have also been used but lower electrical properties were obtained. Conventional sintering is a time-consuming process to obtain highly densified ceramics. Microwave heating generally allows decreasing sintering time. However, few articles deal with the influence of this technic on the electrical properties of BCTZ. Sun *et al.* compared samples obtained by solid-state and hydrothermal routes and sintered by micro-wave [13]. Mane *et al.* investigated the

effect of conventional and microwave sintering on samples obtained by the coprecipitation method [14]. The benefit of this sintering process has also been demonstrated for pure barium titanate [15,16]. Typically, the d_{33} piezoelectric constant of BaTiO_3 could be improved from 160 pC/N for pellets obtained by conventional sintering to 350 pC/N for samples obtained by microwave sintering [17].

Thus, the aim of the present work is to study the influence of microwave sintering on the electrical properties of $\text{Ba}_{0.85}\text{Ca}_{0.15}\text{Ti}_{0.90}\text{Zr}_{0.10}\text{O}_3$.

2. Materials and methods

$\text{Ba}_{0.85}\text{Ca}_{0.15}\text{Ti}_{0.90}\text{Zr}_{0.10}\text{O}_3$ was prepared by conventional solid-state route using BaCO_3 (Alfa Aesar, 99 %), CaCO_3 (Alfa Aesar, 99.8 %), TiO_2 (Sigma Aldrich, 99 %), and ZrO_2 (Sigma Aldrich, 99.99 %) as starting materials. These powders were mixed in stoichiometric ratios by attrition milling in alcoholic medium during 4 h. The slurry was dried and then calcined at 1300 °C during 2 h. The calcined powder was attrition milled once more in alcoholic medium during 4 h. The obtained powder was compacted into 13 mm in diameter and 2 mm thick pellets by uniaxial pressing followed by cold isostatic pressing. Samples were sintered by two sintering methods: conventional and microwave sintering. Conventional sintering (CS) was conducted at 1400 °C for 3 h.

* Corresponding author.

E-mail address: yannick.lorgouilloux@uphf.fr (Y. Lorgouilloux).

Table 1
Relative density and grain size for samples sintered by CS and MWS for different dwell times.

Samples	Relative density (%)	Grain size (μm)
CS_3H	95.1 \pm 0.4	42.1 \pm 14.2
MWS_5 min	93.4 \pm 1.3	9.0 \pm 0.9
MWS_10 min	93.3 \pm 0.6	11.3 \pm 1.3
MWS_15 min	94.6 \pm 1.0	12.2 \pm 1.8
MWS_20 min	94.1 \pm 0.6	14.9 \pm 2.3
MWS_25 min	94.8 \pm 0.4	16.1 \pm 2.4
MWS_30 min	94.7 \pm 0.8	17.3 \pm 3.0
MWS_40 min	94.8 \pm 0.8	18.4 \pm 3.0
MWS_50 min	94.7 \pm 0.4	22.6 \pm 4.4
MWS_60 min	95.0 \pm 0.6	24.1 \pm 4.8

Concerning microwave sintering (MWS), the same temperature was chosen and different dwell times (from 5 to 60 min) were applied. Microwave sintering was carried out by using a microwave generator (Sairem GMP 20 K SM, 2.45 GHz) that applies a variable power up to 2 kW along a standard WR340 rectangular waveguide (section of $86.36 \times 43.18 \text{ mm}^2$) equipped with a water circulator and ended by a TE10m rectangular microwave cavity. The cavity can be tuned in TE10m ($m = 4$ or 5) modes by setting the length between the coupling iris and the short circuit piston. The resonance is manually tuned to be maximal with a stub and the temperature is adjusted by varying the incident power. The sample was placed into an alumina-silicate thermal insulation box (Fiberfrax Duraboard®) that is microwave transparent. An annular SiC susceptor was placed all around the sample, into the box, in order to initiate the microwave heating. The whole assembly was set in the middle of the cavity. In this study, the cavity was tuned in TE105 mode involving mostly the electric field (E mode). The temperature was determined by using an infrared pyrometer (Ircon, Modline5, 350–2000 °C) vertically positioned on the top of the cavity and focused directly on the sample surface.

Experimentally, a power of 200 W was selected to initiate the sample heating. Then, the sample was heated up by raising the power up to 400 W to reach the sintering temperature within 7 min. The temperature was maintained for the selected duration, and the sample was then cooled down to room temperature (RT) within 3 min by cutting down the power. The samples density was determined using the

Archimedes method. The microstructures were observed using a scanning electron microscope (Jeol-JCM-6000). The line intercept method was used for grain size determination. The crystalline structures were determined by X-Ray diffraction using the Cu-K α radiation (Panalytical-X'PERT Pro). Poling was carried out in silicon oil by applying a 3 kV/mm DC-field at room temperature during 30 min and d_{33} was measured 24 h later with a piezometer (Piezotest-PM200). The dielectric properties were measured at 1 kHz on poled samples from 0 °C to 130 °C with a heating rate of 0.1 °C/min by using a climatic chamber (Vötsch-VT 4002).

The ferroelectric cycles were measured using a commercial device (AixPES, Aixact) fitted with a piezo sample holder unit (PSU, 25–200 °C) and a laser interferometer allowing to determine the strain/field piezoelectric cycles. The measurements were carried out at 50 mHz using a triangular sawtooth signal. The converse piezoelectric coefficients d_{33}^* were calculated using a linear fit of the displacement/voltage curves.

3. Results

3.1. Microstructure and densification

Table 1 summarizes the relative density and the grain size measured for samples obtained by CS and MWS. A relative density around 94 % of the theoretical density (5.68 g/cm^3) was measured for all samples obtained by CS and MWS. Microstructures of BCTZ ceramics sintered by both technics are shown in Fig. 1. Microstructures with heterogeneous grain sizes were obtained whatever the sintering method. It is most probably due to the bimodal grain size distribution observed in the powder (after the second ball milling). In the ground powder, the grain size of the first population was around 100 nm and the second around 1 μm . A grain size of $42.1 \pm 14.2 \mu\text{m}$ was measured on the sample obtained by conventional sintering. Thanks to the microwave sintering, it was possible to obtain a finer microstructure due to the shorter thermal treatment times [18]. The grain size increased with the duration of dwell time from $9.0 \pm 0.9 \mu\text{m}$ for 5 min to $24.1 \pm 4.8 \mu\text{m}$ for 60 min.

3.2. X-ray diffraction

XRD patterns obtained for pellets sintered by both sintering methods and for different microwave sintering dwell times are shown in

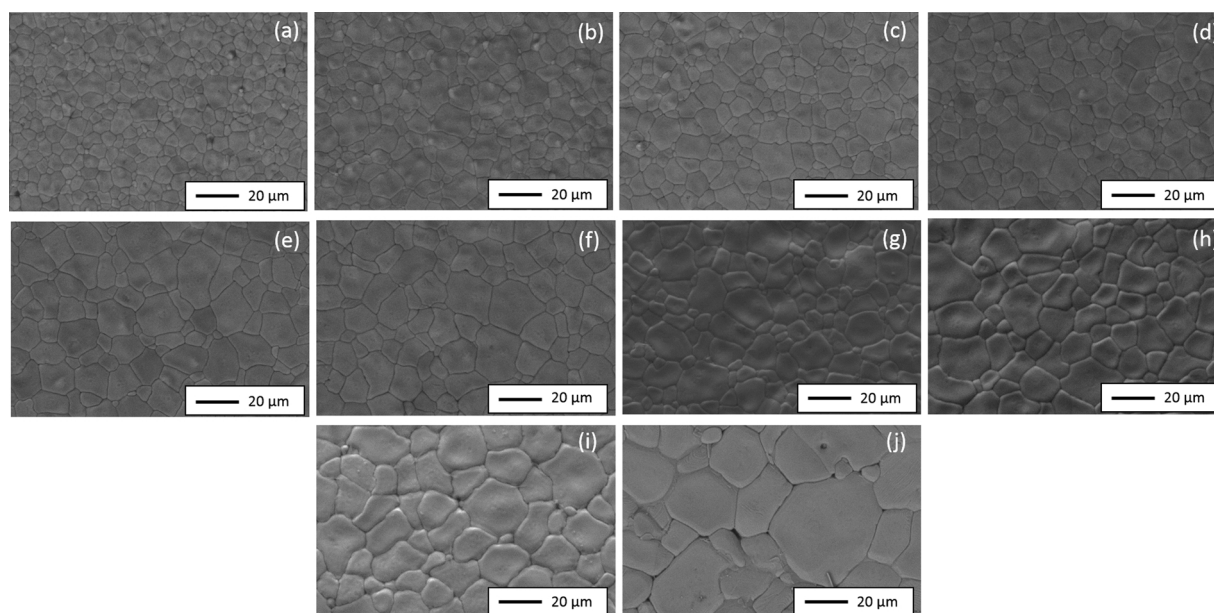


Fig. 1. SEM images of BCTZ ceramics sintered by MWS at 1400 °C during (a) 5, (b) 10, (c) 15, (d) 20, (e) 25, (f) 30, (g) 40, (h) 50 and (i) 60 min, (j) SEM image of a BCTZ ceramic sintered by CS at 1400 °C during 3 h.

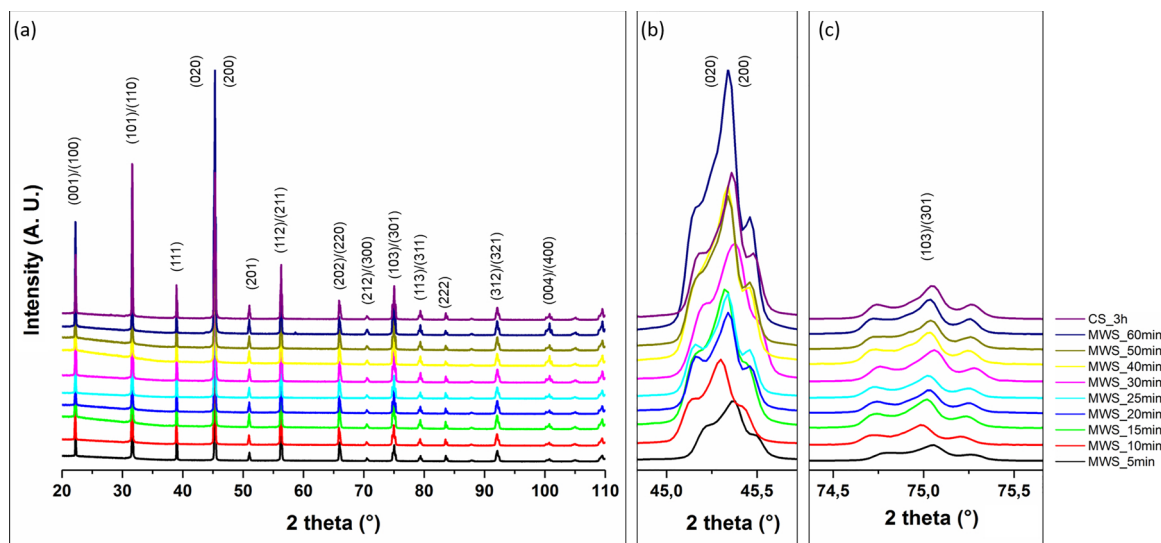


Fig. 2. XRD patterns of samples obtained by CS and MWS. From bottom to top: samples obtained by MWS during 5, 10, 15, 20, 25, 30, 40, 50 and 60 min and by CS during 3 h. (a) Patterns over the full 2 theta range. (b) Zoom on the (45–46 °) 2 theta range. (c) Zoom on the (74.5–75.5 °) 2 theta range. XRD patterns are indexed as a tetragonal structure using JCPDS No. 00-005-0626.

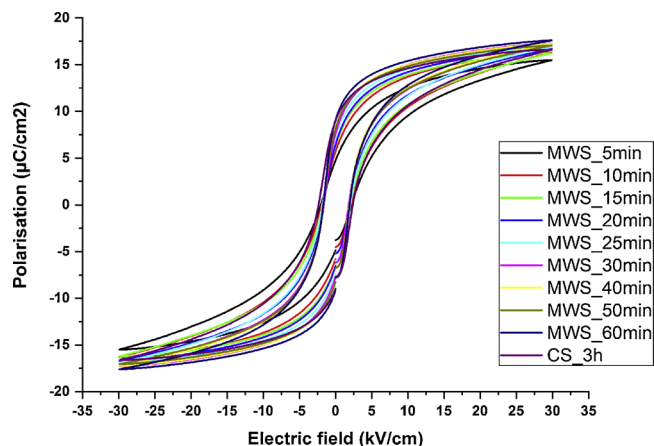


Fig. 3. Polarization–Electric field (P-E) hysteresis loops measured at 3 kV/mm for samples sintered by CS and MWS with different dwell times.

Fig. 2(a). All samples exhibited perovskite crystal structure and no secondary phases were detected. For all the samples, attempts to perform structural refinement by a single perovskite phase were unsuccessful. Differences concerning the asymmetry of some peaks agree with the presence of several crystalline structures and similar XRD patterns can be found in the literature [6,19]. Haugen *et al.* investigated the BCT-BTZ system and evidenced that XRD patterns can be fitted only

using a mix of rhombohedral (R3m) and tetragonal (P4mm) structures [20]. Brajesh *et al.* evidenced for the coexistence of three phases: rhombohedral (R3m) + orthorhombic (Amm2) + tetragonal (P4mm) for the 50BCT-50BTZ composition [21]. They also evidenced that the amount of these different phases depends on the history of the samples: XRD patterns were not the same for annealed, stressed or poled samples. Our results agree well with such a phase coexistence. Indeed, we observed some modification concerning the asymmetry of the diffraction peaks by increasing the dwell time of the microwave sintering. For example, the peaks at 45 ° and at 75 °, corresponding to the (002)/(200) and (103)/(301)/(310) tetragonal peaks, respectively, are modified (Fig. 2(b) and (c)). The increase of the dwell time for MWS seems to affect the amount of each crystalline structure according to the variation of the intensity of some diffraction peaks. Further experiments are in progress in order to determine the amount of each phase as a function of sintering time.

3.3. Ferroelectric and piezoelectric properties

Electrical properties were also investigated by measuring the Polarization–Electric field (P-E) hysteresis loops (Fig. 3). The coercive field does not seem to have been affected by the increase of sintering time (Fig. 4). At the opposite, the remnant and saturation polarizations increased with the dwell time. The remnant polarization increased from 4.8 $\mu\text{C}/\text{cm}^2$ to 15.5 $\mu\text{C}/\text{cm}^2$ for dwell times of 5 and 60 min respectively. The grain growth was thus beneficial for the ferroelectric properties.

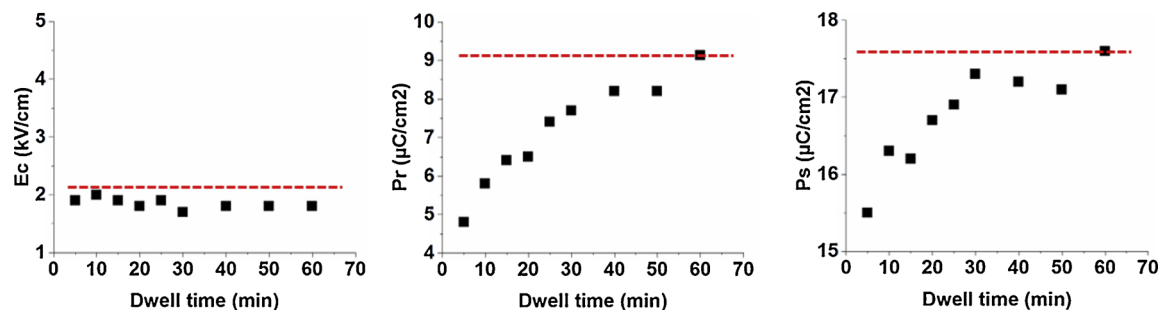


Fig. 4. Ferroelectric properties measured at 3 kV/mm for samples sintered by MWS with different dwell times (the dashed lines show values obtained for the CS sample).

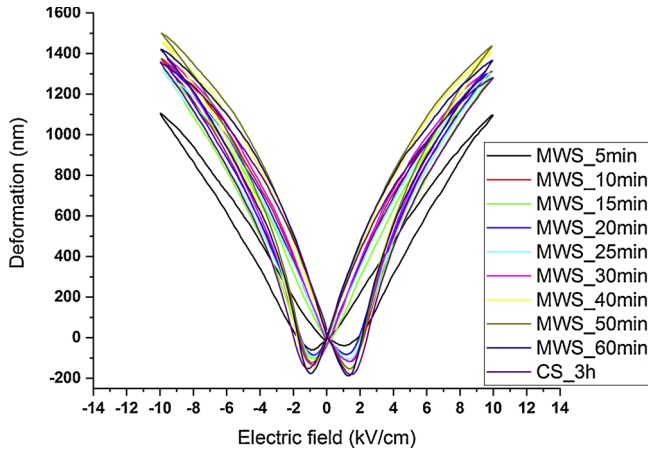


Fig. 5. Displacement hysteresis loops measured at 1 kV/mm for samples sintered by CS and MWS with different dwell times.

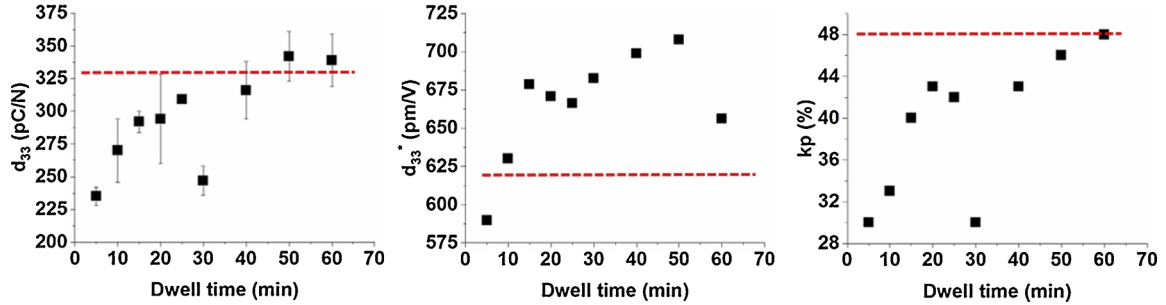


Fig. 6. Piezoelectric coefficients in direct effect (d_{33}) and converse effect (d_{33}^*) and electromechanical coupling factor (k_p) of samples sintered by MWS with different dwell times (the dashed lines show values obtained for the CS sample).

Electrical breakdown appeared during the poling step for pellets sintered by microwave. This phenomenon was due to the stress induced by the high rates of heating and cooling for microwave sintering. An annealing at 1000 °C during 1 h in a conventional oven was required to release the stress inside the samples. After annealing all samples could be poled by a DC electric field, excepted for the pellets sintered by microwave with a 30 min dwell time.

The converse piezoelectric constant values have been determined

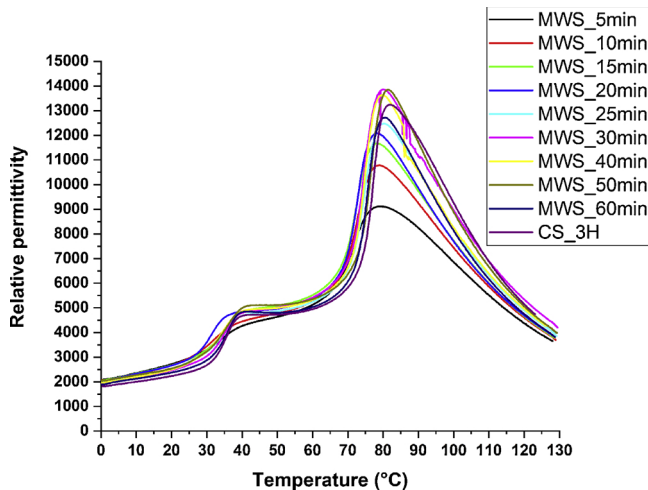


Fig. 7. Temperature dependence of the relative permittivity at 1 kHz for samples sintered by CS and MWS with different dwell times.

from the displacement hysteresis loops (Fig. 5). For samples sintered by conventional method, no annealing was required, and very good piezoelectric properties were measured: $d_{33} = 333 \pm 3$ pC/N and $d_{33}^* = 622$ pm/V. The evolution of the piezoelectric (direct and converse effects) properties and the electromechanical coupling factor with the increase of the dwell time for MWS is presented in Fig. 6.

By MWS, the d_{33} piezoelectric constant increased with the thermal treatment duration, reaching 342 ± 19 pC/N for a 50 min dwell time. Further increase of dwell time (60 min) did not lead to any change of d_{33} . Surprisingly, a d_{33} value of 247 ± 11 pC/N was measured for the sample sintered by microwave with 30 min of dwell time. This low value did not follow the trend observed for other durations and can be explained by the fact that electrical breakdown had happened during the poling even with the annealing step.

The d_{33} values obtained for the longer MWS treatments are similar to those obtained by CS (even slightly higher).

However, due to the fast sintering allowed by MWS, these good d_{33} piezoelectric constant values could be obtained with a grain size almost twice as small: 22.6 ± 4.4 μm was measured for the 50 min MWS samples compared to 42.1 ± 14.2 μm measured for samples obtained

by CS. Grain size does not seem to have much influence on the piezoelectric constant here.

Concerning the converse piezoelectric constant (d_{33}^*), the same tendency could be observed. Values increased from 589 pm/V to 656 pm/V for dwell times from 5 to 60 min. It has to be noted that the highest d_{33}^* value was obtained for a 50 min dwell time, with 708 pm/V and then slightly decreased when reaching 60 min ($d_{33}^* = 656$ pm/V). Moreover, for the converse effect, properties of the MWS samples are higher than for CS samples, even for sintering durations as short as 15 min. For these properties, grain size seems to be an important parameter. Further characterizations may be useful to discriminate among the influence of grain sizes and domain sizes, but these were not conducted yet.

By increasing the dwell time of MWS, the electromechanical coupling factor was enhanced from 30 % for 5 min to 48 % for 60 min dwell time. A similar value (48 %) was measured for pellets sintered by conventional method.

3.4. Dielectric properties and Curie temperature

Dielectric properties were measured for each sample and are presented Figs. 7 and 8. Relative permittivity and dielectric losses were measured at 1 kHz and at room temperature. The dielectric losses were lower than 3.5 % and were not affected by the sintering method nor by the dwell time. Concerning the relative permittivity, the values decreased from 2962 for a 5 min dwell time to 2554 for a 60 min dwell time.

The Curie temperature was around 80 °C whatever the sintering method and the dwell time (for MWS). Similar values could be found in the literature. Wang *et al.* and Srinivas *et al.* have measured respectively

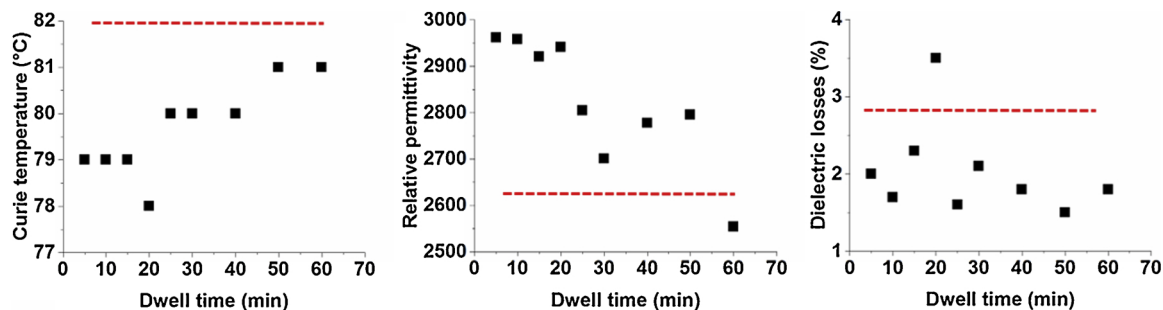


Fig. 8. Dielectric properties of samples sintered by MWS with different dwell times (the dashed lines show values obtained for the CS sample).

a Curie temperature of 85 °C [7] and 82 °C [22] for the same material.

4. Conclusion

This study demonstrated that BCTZ piezoelectric ceramics can be obtained by microwave sintering, thus reducing the thermal treatment duration (including heating, dwell time and cooling) from 12.5 h down to 1.5 h. As expected, the sintering method has an influence on the microstructure of ceramic samples, the microstructure being finer with MWS than with CS, which is usually deleterious to piezoelectric properties. However, here microwave sintering allowed obtaining ceramics with d_{33} piezoelectric constant as high as those of pellets obtained by conventional sintering. The converse piezoelectric constant values were even higher for MWS than for CS. Lead free piezoceramics with high piezoelectric properties ($d_{33} > 330$ pC/N) were reported [23–25], but the present study is the first example of BCTZ ceramics obtained by combining the solid state route for powder synthesis and microwave sintering showing so good electrical properties. Moreover, as MWS leads to samples with finer microstructures better mechanical properties are expected with this technique.

Declaration of Competing Interest

The authors declare that they have no known competing financial interests or personal relationships that could have appeared to influence the work reported in this paper.

Acknowledgment

This work was supported by the “Direction Générale de l’Armement” – Ministère des Armées and the Région Hauts-de-France.

References

- [1] G. Lockitch, Perspectives on lead toxicity, *Clin. Biochem.* 26 (1993) 371–381, [https://doi.org/10.1016/0009-9120\(93\)90113-K](https://doi.org/10.1016/0009-9120(93)90113-K).
- [2] L. Patrick, Lead toxicity, a review of the literature. Part 1: exposure, evaluation, and treatment, *Altern. Med. Rev.* 11 (2006) 2–22.
- [3] European Commission, Regulation (EC) No 1907/2006 of the European Parliament and of the Council of 18 December 2006 Concerning the Registration, Evaluation, Authorisation and Restriction of Chemicals (REACH), Establishing a European Chemicals Agency, Amending Directive 1999/45/EC and Repealing Council Regulation (EEC) No 793/93 and Commission Regulation (EC) No 1488/94 as well as Council Directive 76/769/EEC and Commission Directives 91/155/EEC, 93/67/EEC, 93/105/EC and 2000/21/EC, *Off. J. Eur. Union* 396 (2006) 374–375.
- [4] EU-Directive 2011/65/EC: restriction of the use of certain hazardous substances in electrical and electronic equipment (RoHS), *Off. J. Eur. Union* (2011) 88–110.
- [5] Directive 2012/19/EU of the European Parliament and of the Council of 4 July 2012 on Waste Electrical and Electronic Equipment (WEEE) Text with EEA Relevance, 2012. <http://data.europa.eu/eli/dir/2012/19/oj/eng>, (Accessed 9 August 2018).
- [6] W. Liu, X. Ren, Large piezoelectric effect in Pb-free ceramics, *Phys. Rev. Lett.* 103 (2009), <https://doi.org/10.1103/PhysRevLett.103.257602>.
- [7] P. Wang, Y. Li, Y. Lu, Enhanced piezoelectric properties of $(\text{Ba}_{0.85}\text{Ca}_{0.15})(\text{Ti}_{0.9}\text{Zr}_{0.1})\text{O}_3$ lead-free ceramics by optimizing calcination and sintering temperature, *J. Eur. Ceram. Soc.* 31 (2011) 2005–2012, <https://doi.org/10.1016/j.jeurceramsoc.2011.04.023>.

- [8] J.P. Praveen, K. Kumar, A.R. James, T. Karthik, S. Asthana, D. Das, Large piezoelectric strain observed in sol-gel derived BZT–BCT ceramics, *Curr. Appl. Phys.* 14 (2014) 396–402, <https://doi.org/10.1016/j.cap.2013.12.026>.
- [9] E. Chandrakala, J. Paul Praveen, B.K. Hazra, D. Das, Effect of sintering temperature on structural, dielectric, piezoelectric and ferroelectric properties of sol-gel derived BZT–BCT ceramics, *Ceram. Int.* 42 (2016) 4964–4977, <https://doi.org/10.1016/j.ceramint.2015.12.009>.
- [10] G.K. Sahoo, R. Mazumder, Low temperature synthesis of $\text{Ba}(\text{Zr}_{0.2}\text{Ti}_{0.8})\text{O}_3-0.5(\text{Ba}_{0.7}\text{Ca}_{0.3})\text{TiO}_3$ nanopowders by solution based auto combustion method, *J. Mater. Sci. Mater. Electron.* 25 (2014) 3515–3519, <https://doi.org/10.1007/s10854-014-2048-2>.
- [11] S. Hunpratub, S. Phokha, S. Maensiri, P. Chindaprasit, Dielectric and piezoelectric properties of lead-free $\text{Ba}_{0.85}\text{Ca}_{0.15}\text{Ti}_{0.9-x}\text{Zr}_{0.1}\text{Cu}_x\text{O}_3$ ceramics synthesized by a hydrothermal method, *Appl. Surf. Sci.* 369 (2016) 334–340, <https://doi.org/10.1016/j.apsusc.2016.01.273>.
- [12] Y. Liu, Y. Pu, Z. Sun, Enhanced relaxor ferroelectric behavior of BCZT lead-free ceramics prepared by hydrothermal method, *Mater. Lett.* 137 (2014) 128–131, <https://doi.org/10.1016/j.matlet.2014.08.138>.
- [13] Z. Sun, Y. Pu, Z. Dong, Y. Hu, P. Wang, X. Liu, Z. Wang, Impact of fast microwave sintering on the grain growth, dielectric relaxation and piezoelectric properties on $\text{Ba}_{0.18}\text{Ca}_{0.02}\text{Ti}_{0.09}\text{Zr}_{0.10}\text{O}_3$ lead-free ceramics prepared by different methods, *Mater. Sci. Eng. B* 185 (2014) 114–122, <https://doi.org/10.1016/j.mseb.2014.02.016>.
- [14] S.M. Mane, P.M. Tirmali, S.L. Kadam, D.J. Salunkhe, C.B. Kolekar, S.B. Kulkarni, Microwave-assisted sintering and improved dielectric, ferroelectric properties of $0.5[(\text{Ba}_{0.7}\text{Ca}_{0.3})\text{TiO}_3]-0.5[\text{Ba}(\text{Zr}_{0.2}\text{Ti}_{0.8})\text{O}_3]$ lead-free ceramics, *Appl. Ceram. Int.* 116 (2017) 325–332, <https://doi.org/10.1080/17436753.2017.1316046>.
- [15] S.O. Leontsev, R.E. Eitel, Progress in engineering high strain lead-free piezoelectric ceramics, *Sci. Technol. Adv. Mater.* 11 (2010), <https://doi.org/10.1088/1468-6996/11/4/044302>.
- [16] H. Takahashi, Y. Numamoto, J. Tani, K. Matsuta, J. Qiu, S. Tsurekawa, Lead-free barium titanate ceramics with large piezoelectric constant fabricated by microwave sintering, *J. Appl. Phys.* 45 (2006) L30–L32, <https://doi.org/10.1143/JJAP.45.L30>.
- [17] S.-F. Liu, I.R. Abothu, S. Komarneni, Barium titanate ceramics prepared from conventional and microwave hydrothermal powders, *Mater. Lett.* 38 (1999) 344–350, [https://doi.org/10.1016/S0167-577X\(98\)00187-6](https://doi.org/10.1016/S0167-577X(98)00187-6).
- [18] D.K. Agrawal, Microwave processing of ceramics, *Curr. Opin. Solid State Mater. Sci.* 3 (1998) 480–485, [https://doi.org/10.1016/S1359-0286\(98\)80011-9](https://doi.org/10.1016/S1359-0286(98)80011-9).
- [19] D.S. Keeble, F. Benabdallah, P.A. Thomas, M. Maglione, J. Kreisel, Revised structural phase diagram of $(\text{Ba}_{0.7}\text{Ca}_{0.3})\text{TiO}_3$ – $(\text{BaZr}_{0.2}\text{Ti}_{0.8}\text{O}_3)$, *Appl. Phys. Lett.* 102 (2013), <https://doi.org/10.1063/1.4793400> 092903.
- [20] A. Bjørnetun Haugen, J.S. Forrester, D. Damjanovic, B. Li, K.J. Bowman, J.L. Jones, Structure and phase transitions in $0.5(\text{Ba}_{0.7}\text{Ca}_{0.3}\text{TiO}_3)$ – $0.5(\text{BaZr}_{0.2}\text{Ti}_{0.8}\text{O}_3)$ from –100 °C to 150 °C, *J. Appl. Phys.* 113 (2013), <https://doi.org/10.1063/1.4772741> 014103.
- [21] K. Brajesh, K. Tanwar, M. Abebe, R. Ranjan, Relaxor ferroelectricity and electric-field-driven structural transformation in the giant lead-free piezoelectric $(\text{Ba}, \text{Ca})(\text{Ti}, \text{Zr})\text{O}_3$, *Phys. Rev. B* 92 (2015), <https://doi.org/10.1103/PhysRevB.92.224112>.
- [22] A. Srinivas, R.V. Krishnaiah, V.L. Niranjani, S.V. Kamat, T. Karthik, S. Asthana, Ferroelectric, piezoelectric and mechanical properties in lead free $0.5\text{Ba}(\text{Zr}_{0.2}\text{Ti}_{0.8})\text{O}_3-0.5(\text{Ba}_{0.7}\text{Ca}_{0.3})\text{TiO}_3$ electroceramics, *Ceram. Int.* 41 (2015) 1980–1985, <https://doi.org/10.1016/j.ceramint.2014.08.127>.
- [23] W. Bai, D. Chen, P. Li, B. Shen, J. Zhai, Z. Ji, Enhanced electromechanical properties in -textured $(\text{Ba}_{0.85}\text{Ca}_{0.15})(\text{Zr}_{0.1}\text{Ti}_{0.9})\text{O}_3$ lead-free piezoceramics, *Ceram. Int.* 42 (2016) 3429–3436, <https://doi.org/10.1016/j.ceramint.2015.10.139>.
- [24] J. Wu, D. Xiao, W. Wu, Q. Chen, J. Zhu, Z. Yang, J. Wang, Composition and poling condition-induced electrical behavior of $(\text{Ba}_{0.85}\text{Ca}_{0.15})(\text{Ti}_{1-x}\text{Zr}_x)\text{O}_3$ lead-free piezoelectric ceramics, *J. Eur. Ceram. Soc.* 32 (2012) 891–898, <https://doi.org/10.1016/j.jeurceramsoc.2011.11.003>.
- [25] J. Wu, D. Xiao, W. Wu, J. Zhu, J. Wang, Effect of dwell time during sintering on piezoelectric properties of $(\text{Ba}_{0.85}\text{Ca}_{0.15})(\text{Ti}_{0.90}\text{Zr}_{0.10})\text{O}_3$ lead-free ceramics, *J. Alloys Compd.* 509 (2011) L359–L361, <https://doi.org/10.1016/j.jallcom.2011.08.024>.